INTERNATIONAL ATOMIC ENERGY AGENCY
UNITED NATIONS EDUCATIONAL, SCIENTIFIC AND CULTURAL ORGANIZATION
INTERNATIONAL CENTRE FOR THEORETICAL PHYSICS
I.C.T.P., P.O. BOX 586, 34100 TRIESTE, ITALY, CABLE: CENTRATOM TRIESTE

SMR/534-16

ICTP/WMO WORKSHOP ON EXTRA-TROPICAL AND TROPICAL
LIMITED AREA MODELLING
22 October - 3 November1990

"Sensitivity Tests Over Kenya Using a 2-Dimensional Model"

A. E. OKEYO
Department of Meteorology
University of Nairobi
Nairobi
Kenya

Abstract

Four numerical experiments are conducted to study mesoscale flows over Kenya using a two-dimensional numerical model. The experiments cover a variety of phenomena that influence weather activity over Kenya during the dry season. The control experiment utilizes the explicit moisture scheme. In comparison the simulations with those from a cumulus parametrization scheme it is found that the cumulus parametrization scheme simulations are closer to observed situation than those of the explicit scheme. In another experiment using a passive moisture scheme (in which moisture was not allowed to interact with other variables) it was shown that cumulus convection plays an important role in the strengths and locations of the mesoscale flows.

In a fourth experiment in which both Lake Victoria and the Indian ocean were excluded from the run, it was shown that Lake Victoria circulation plays an important role in the occurrence of the hailstorms or thunderstorms over the Kenya highlands.

1. INTRODUCTION

Over most parts of the tropics in general and over Kenya in particular weather systems depend to a large extent on the small scale systems such as lake/sea and land breezes, mountain flows and the generally prevalent tropical convective instability. A major objective of this study is to examine the mesoscale systems that are responsible for weather patterns over Kenya. A lot of research has been done along this line in many parts of the world. Most of such research has been done in the midlatitudes where the Coriolis effect has strong influence on the atmospheric flow field. In this study the model is formulated for a non-rotating plane (f=0). The neglect of the earth's rotation in a mesoscale flow model is considered a valid first approximation, especially in the tropical regions where the local Coriolis parameter is much smaller than the Doppler-Shifted frequency and therefore the Rossby number exceeds unity. Some of the research work done on this field include Estoque (1961, 1962), Moroz (1967), Pearce (1955, 1962) and Okeyo (1982). These studies used simple models to simulate some of the mesoscale phenomena like lake/sea and land breezes. They used dry models and therefore were only able to simulate the general flow patterns of these systems.

Despite the simplicity of the models, the researchers were able to make concrete estimations about the future behaviour of these mesoscale systems.

Recently, more sophisticated models have been formulated which incorporate different types of parameterization schemes like, cumulus convection, radiative effects etc. These types of parameterizations have enable researchers to simulate both mesoscale and convective-scale systems more accurately. Such studies include those of Anthes (1977), Anthes and Warner (1978), Hsie (1983) and Okeyo (1987).

In a numerical model especially of a mesoscale or convective-scale nature, the parameterization of the planetary boundary layer (PBL) is a significant feature which must be properly incorporated. This study considers the variation in the surface parameters such as albedo, moisture availability, roughness length etc. It is also important to note that a realistic parameterization of heat, moisture, and momentum fluxes due to convective scale processes is of primary significance for numerical models of the interactions between mesoscale and convective-scale systems. Some of these models with realistic parameterizations of these fluxes include those of Anthes (1977), Anthes and Warner (1978), Emmanuel (1982), Kuo and Anthes (1984a, b, c) and Okeyo (1987). In this study the fluxes are computed using the method advanced by Anthes and Warner (1978).

In East Africa some of the observational and numerical studies done show that mesoscale systems are responsible for most of the weather activities over this region (Flohn, 1970, Frankfurt, 1972 Sansom and Gichuiya, 1971, Chaggar, 1977, Asnani and Kinuthia, 1979, and Okeyo 1982, 1987).

This study is concerned with the development of convective-scale and mesoscale flows and the interactions between the two scales in the occurrence of weather activities over Kenya. Okeyo (1982) used a two-dimensional numerical model to simulate land and sea breezes over Kenya. His results showed strong convergence over the Kenya highlands during daytime and over Lake Victoria at night. These findings agreed quite well with the occurrence of thunderstorms/hailstorms over the Kenya highlands during daytime and thunderstorms and showers over the lake at night. In another study, Okeyo (1987), the author showed that Lake Victoria breeze contributes most of the moisture and energy necessary for the high frequency of hailstorms over the Kenya highlands.

2. THE NUMERICAL SCHEME

The dynamical frame is taken from Anthes and Warner (1978), Keyser and Anthes (1982) and Hsie (1983). Anthes and Warner (1978) used a one-dimensional cloud model scheme in their two-dimensional version of the model. While Hsie (1983) used a two-dimensional numerical explicit moisture model to compute frontal circulations in a moist atmosphere. These models were formulated in the middle latitudes where there is strong influence of the earth's rotation i.e. the Coriolis term was significant. They also used Lambert conformal map coordinates. In order to adapt the numerical scheme to an equatorial atmosphere, the Coriolis parameter was taken to be a constant at zero and a Mercator conformal map coordinates assumed.

2.1 The Dry Model

The dry version of the numerical scheme is described in Anthes and Warner (1978) and Hsie (1983). It is a hydrostatic and compressible primitive equation (PE) model. The grid system is staggered both horizontally and vertically. The vertical coordinate is a normalised pressure system given by

$$\sigma = \frac{p - p_t}{p^*} \tag{1}$$

where $p^* = p_s - p_t$

and p_s is pressure at surface and p_t is pressure at top of model.

Using the climatology of the region, the equations of motion, heat and continuity are given as:

$$\frac{\partial p^* u}{\partial t} = -\frac{\partial p^* uu}{\partial x} - \frac{\partial p^* u\sigma}{\partial \sigma} - \frac{RT}{(1+p_t / p^*\sigma)} \frac{\partial p^*}{\partial x} - p^* \frac{\partial \varphi}{\partial x} + fp^* v + p^* F_H u + p^* F_V u \tag{2}$$

$$\frac{\partial p^* v}{\partial t} = -\frac{\partial p^* uv}{\partial x} - \frac{\partial p^* v\sigma}{\partial \sigma} - p^* fu + p^* F_H v + p^* F_V u \tag{3}$$

$$\frac{\partial p^* T}{\partial t} = -\frac{\partial p^* Tu}{\partial x} - \frac{\partial p^* T\sigma}{\partial \sigma} + \frac{RT\omega}{Cp(\sigma + p_t / p^*)} + \frac{p^* Q}{Cp} + p^* F_H T + p^* F_V T \tag{4}$$

$$\frac{\partial p^*}{\partial t} = -\frac{\partial p^* u}{\partial x} - \frac{\partial p^* \sigma}{\partial \sigma} \tag{5}$$

$$\sigma = -\frac{\sigma}{p^*}\frac{\partial p^*}{\partial t} - \frac{1}{p^*}\int_0^{\sigma} \frac{\partial p^* u}{\partial x}\, d\sigma \tag{6}$$

$$\omega = p^* \sigma + \sigma\left(\frac{\partial p^*}{\partial y} + u\frac{\partial p^*}{\partial x}\right) \tag{7}$$

The hydrostatic equation in this scheme is given by:

$$\frac{\partial \varphi}{\partial \ell n\,(\sigma + p_{t/p^*})} = -RT \tag{8}$$

A sufficient condition for the hydrostatic assumption is that the horizontal scale exceeds the vertical scale i.e. $\frac{\Delta z}{\Delta x} < 1$.

The equation of state is given by

$$p = \rho RT \tag{9}$$

In the above scheme, u and v are zonal and meridional components of velocity respectively, σ is the vertical velocity in σ-coordinate system, T is temperature, ρ is density of dry air, ω is the vertical velocity in pressure coordinate system, φ is geopotential, R is the gas constant for dry air, Cp is the specific heat at constant pressure for dry air, f is Coriolis parameter which is assumed equal to zero in this scheme, g is gravitational acceleration, and Q is the diabatic heating rate. The subscript s represents the value at the surface. The F_H and F_v terms are the horizontal and vertical diffusion terms respectively.

2.2 The Moist Scheme

The moist version of the numerical scheme contains additional equations to represent the effects of condensation and evaporation and the associated release of the latent heat of condensation.

2.2.1 The Explicit Scheme

In this scheme three additional equations are needed. These are the explicit prediction of the mixing ratios of water vapour q_v, cloud water q_c, and rainwater q_r as follows:

$$\frac{\partial p^* q_v}{\partial t} = -\frac{\partial p^* q_v u}{\partial x} - \frac{\partial p^* q_v \dot{\sigma}}{\partial \sigma} + p^*(P_{RE}-P_{CON}) + p^* F_H q_v + p^* F_v q_v \qquad (10)$$

$$\frac{\partial p^* q_c}{\partial t} = -\frac{\partial p^* q_c u}{\partial x} - \frac{\partial p^* q_c \dot{\sigma}}{\partial \sigma} - p^*(P_{RA}+P_{RC}-P_{CON}) + p^* F_H q_c + P^* F_v q_c \qquad (11)$$

$$\frac{\partial p^* q_r}{\partial t} = -\frac{\partial p^* q_r u}{\partial x} - \frac{\partial p^* q_r \dot{\sigma}}{\partial \sigma} + p^*(P_{RA}+P_{RC}-P_{RE}) - g\frac{\partial \rho q_r v_t}{\partial \sigma} + p^* F_H q_r \qquad (12)$$

where P_{RA} is the accretion of cloud droplets by raindrops, P_{RC} is the autoconversion of cloud droplets to raindrops, P_{RE} is the evaporation of raindrops, P_{CON} is the condensation of water vapour or evaporation of cloud droplets, and v_t is the mass-weighted mean terminal velocity of raindrops.

The formulation for P_{RA} and P_{RE} follow Orville and Kopp (1977), P_{RC} follows Kessler (1969), P_{CON} follows Asai (1965), and terminal velocity v_t follows Liu and Orville (1969)

The autoconversion process is given by:

$$P_{RC} = \begin{cases} k_1 (q_c - q_{co}) & q_c \geq q_{co} \\ 0 & q_c < q_{co} \end{cases} \qquad (13)$$

where $k_1 = 10^{-3}$ sec^{-1} and the critical value for the onset of autoconversion q_{co} is 0.5 g kg^{-1}.

As described by Hsie (1983), the P_{CON} term is computed diagnostically which has the advantage of a one-step computation, no iteration is needed. First the mixing ratios of water vapour and cloud water are calculated without the P_{CON} term. Then supersaturation or undersaturation with cloud water (evaporation) is checked. A one-step adjustment is then used to compute the P_{CON} term. The north-south boundary conditions for cloud water and rainwater are the same as those for u and v i.e. the y gradients are zero on pressure surfaces.

The effect of moisture is to add correction terms to the thermodynamic equation (4), the hydrostatic equation (8) and the ideal gas law (9) as follows:

$$\frac{\partial p^* T}{\partial t} = -\frac{\partial p^* T u}{\partial x} - \frac{\partial p^* T \dot{\sigma}}{\partial \sigma} + \frac{R T_v \omega}{C_{pm}(\sigma + p_t/p^*)} + \frac{p^* L_v (P_{CON}-P_{RE})}{C_{pm}} + p^* F_H T + p^* F_v T \qquad (14)$$

$$\frac{\partial \varphi}{\partial \ell n(\sigma + p_t/p^*)} = -\frac{R T_v}{\left[1 + \frac{q_c + q_r}{1 + q_v}\right]} \qquad (15)$$

$$p = \rho R T_v \qquad (16)$$

where $Tv = T(1 + 0.608\, q_v)$ (17)

is the virtual temperature, ρ is the density for moist air,

$$C_{pm} = C_p (1 + 0.8\, q_v) \qquad (18)$$

is the specific heat at constant pressure for moist air, L_v is the latent heat of condensation, which is constant in this model. The effects of liquid water in the thermodynamic equation and ideal gas laws are neglected here, however, the effect of water loading on the hydrostatic equation is considered. From the hydrostatic equation, (15), when liquid water exists, the geopotential height is decreased. The effect on the wind field may be small, but a small change in the horizontal wind field can significantly affect the divergence, and convection is closely related to the divergence patterns.

The initial relative humidity for the explicit scheme (which is taken as the control experiment) is arbitrarily specified to be 98% throughout the domain to ensure early development of convection and to save computer time. Any water vapour in excess of the critical humidity (condensation threshold) is condensed. The critical relative humidity for the control simulation is taken as 100%.

The fallout term is diagnosed after all other terms are calculated, to ensure that the maximum rain water fallen out of a grid-point column is the rain water at that point. A high frequency oscillation in the rainwater field can occur in the lowest model layer. The process most significantly affected by this oscillation is the evaporation of rainwater (P_{RE}). Because of the high relative humidity, the evaporation of rain water is not an important factor in these simulations. In addition, it only affects the lowest model layer. Because the liquid water fields show greater temporal variability, the smoothing coefficient in the filter (Asselin, 1972) for these two fields doubled compared with the coefficients for u, v, T, p* and q_v.

When water vapour is the only prognostic variable all of the condensed water is removed as precipitation. The condensation term (P_{CON}) is computed using the same procedure mentioned above (Asai, 1965), except that no re-evaporation of liquid water is allowed. When the prognostic equation for rainwater is neglected, mixing ratio of cloud water in excess of 0.55 g kg^{-1} is removed as precipitation. This number is arbitrarily prescribed.

2.2.2 The Cumulus Parameterization Scheme

In the numerical model used in this study the cumulus parameterization scheme utilizes the one-dimensional cloud model by Anthes (1977). In this scheme, the cumulus parameterization is evaluated when the atmosphere is conditionally unstable and the horizontal moisture convergence in the lower troposphere exceeds a critical value. The closure assumption for this scheme is that the latent heat released is proportional to the total moisture convergence

$$M_t = -\frac{1}{g}\int_0^1 \nabla\cdot\nabla^* (p^* q_v)\, d\sigma \qquad (18)$$

The total moisture convergence is separated into two parts. A fraction (1-b) of M_t is precipitated out and the remaining fraction b is redistributed in the vertical column. The fraction b is a function of a mean relative humidity in the column and is estimated by:

$$b = \begin{cases} \left[\frac{(1-RH')}{(1-RH_c)}\right]^n & RH' \geq RH_c \\ 1 & RH' < RH_c \end{cases} \qquad (19)$$

where n=1, $RH_c = 0.5$ and RH' is evaluated as

$$RH' = \frac{\langle q_{vs}(T)\cdot RH\rangle}{\langle q_{vs}(T)\rangle} \qquad (20)$$

The use of RH' rather than relative humidity weights the vertical average of relative humidity according to the ability of the layer to hold water vapour. The $\langle\ \rangle$ represents a vertical average operator:

$$\langle (\ ) \rangle = (\sigma_b - \sigma_u)^{-1} \int_{\sigma_u}^{\sigma_b} (\ )\, d\sigma \qquad (21)$$

where σ_u and σ_b are the sigma levels at cloud top and cloud base respectively. The latent heat and moisture assigned to storage are distributed in the vertical by the distribution function suggested by Anthes (1977). The distribution steady state cloud model (Simpson and Wiggert, 1969) as:

$$N(\sigma) = \frac{C_c^*(\sigma)}{\langle C_c^* \rangle} \qquad (22)$$

and

$$p^* P_{CON} = \frac{(1-b)\, g M_t}{(\sigma_b - \sigma_u)}\, N(\sigma) \qquad (23)$$

where C_c^* is the condensation rate computed from the updraft of model cloud. The distribution function for moisture is weighted by relative humidity and saturation mixing ratio q_{vs}

$$N'(\sigma) = \frac{(1-RH)\, q_{vs}}{\langle (1-RH)\, q_{vs} \rangle} \qquad (24)$$

and

$$\left(\frac{\partial p^* q_v}{\partial t}\right)_{CON} = \frac{g b M_t}{(\sigma_b - \sigma_u)}\, N'(\sigma) \qquad (25)$$

The fractional area, a covered by the precipitating convective clouds is computed as

$$a = \frac{(1-b)\, gM_1}{\int_{\sigma_b}^{\sigma_u} p^* C_c^* d\sigma} \qquad (26)$$

This fractional area is used in computing subgrid, convective fluxes:

$$\overline{\dot{\sigma}'\,\alpha'} = \frac{a(\sigma_c-\sigma)(\alpha_c-\alpha)}{(1-a)} \qquad (27)$$

where α represents any variable and subscript c represents the variable in the cloud. Only cloud-scale heat and moisture fluxes are evaluated in the model. Also, only the cloud updraft is considered here. No explicit evaporation is computed (i.e. P_{CON} is always larger than zero).

2.3 Numerical Techniques

The numerical techniques applied to the scheme include the finite difference scheme (both spatial and temporal) horizontal diffusion, and temporal filtering.

2.3.1 Finite Difference Scheme

The finite difference scheme analog used in this model utilizes the S1 grid technique by Shuman and Hovermale (1968) and discussed by Anthes and Warner (1978). The S1 grid conserves energy exactly. For a complete treatise of the scheme see Anthes and Warner (1978) and Anthes et al (1987).

2.3.2 Temporal Integration Scheme

The time-integration scheme used in this study is similar to that by Brown and Campana (1978). This explicit scheme permits for a time-step nearly equal to twice larger than the conventional leapfrog scheme. The stability of the scheme depends on the computation of the values of p^* and φ at timestep $\tau+1$ before computing the momentum values at timestep $\tau+1$. Then, a weighted average of the values of p^* and φ at timesteps $\tau-1$, and $\tau+1$ are utilized in the pressure gradient force term (2) i.e. in this equation

$$p^* = \eta(p^{*\tau-1} + p^{*\tau+1}) + (1-2\eta)\, p^{*\tau} \qquad (30)$$

with a similar expression for φ. The scheme is stable for $\eta \leq 0.25$ and permits maximum timestep for $\eta = 0.25$. In this study a value of 0.2495 is used.

2.3.3 Diffusion Techniques

In the boundary layer for stable, mechanically driven turbulence or forced convection, the vertical fluxes are computed according to K-theory at all times. The coefficients for transport of momentum and heat K_{mz} and $K_{\theta z}$ are calculated as a function of the local Richardson number R_i:

$$K_m = K_{\theta z} = \begin{cases} K_{zo} + k^2 l^2 \left(\frac{\partial W}{\partial z}\right)\left(\frac{R_{ic}-R_i}{R_{ic}}\right) & R_i < R_{ic} \\ K_{zo} & R_i \geq R_{ic} \end{cases} \qquad (31)$$

where W is the wind speed, l is a constant mixing length, $R_{ic} = 1$ is a critical Richardson number and $K_{zo} = 1\ m^2\ s^{-1}$ permits a weak background mixing and z is the height. In the horizontal, the forms of the horizontal diffusion terms for any variable represented by α are

$$F_{H4}\,\alpha = -K_{H4}\frac{\partial^4 \alpha}{\partial x^4} \qquad \text{(fourth order)}$$

and

$$F_{H2}\,\alpha = K_{H2}\frac{\partial^2 \alpha}{\partial x^2} \qquad \text{(second order)} \qquad (33)$$

with

$$K_{H2} = K_{H0} + K^2\,[(\Delta x)^2\left(\frac{\partial u}{\partial x}\right)^2 + \left(\frac{\partial v}{\partial x}\right)^2] \qquad (34)$$

and

$$K_{H4} = (\Delta x)^2\, H_{H2} \qquad (35)$$

where $k = 0.35$ is a von Karman's constant. In this scheme, however, the horizontal diffusion technique was not applied to the heat and moisture fields.

2.4 Initial and Boundary Conditions

The treatment of initial and boundary conditions in a limited area numerical model is a difficult but a very fundamental aspect of the accuracy of the model. In this study these two aspects of the model are treated considering the phenomena under study and the

equatorial proximity of the study area. The limitations of these conditions are however noted and possible improvements suggested.

2.4.1 Initial Conditions

In the tropics in general and equatorial regions in particular, lack of understanding of the prevailing instability makes it difficult to initialise mesoscale numerical forecast models. Also in mesoscale (limited area) modelling unlike large-scale quasi-geostrophic flow, no scaling of the basic hydrodynamic equations will apply under all meteorological conditions. For example, the release of latent heat by condensation is a secondary effect for planetary flows over short (1-2 days) time periods but varies from being negligible under many conditions to dominant under others. Similarly, non-hydrostatic effects may not be ignored under all situations when the horizontal scale of the disturbance is small compared to the vertical scale.

In this study, however, we recognise that for atmospheric disturbances of these scales, the solutions are often determined more by the local forcing than by the initial disturbance of the particular wave. Following this hypothesis and the geography of the model domain (i.e. surrounded by lake and ocean and a hilly landscape), we started our integrations from a state of rest at 0600 h local time (a time of changeover from nocturnal flow to daytime flow). We further realise that in January, the flow is mainly northeasterly i.e. parallel to the Indian Ocean coast, and hence the large-scale synoptic flow would have negligible influence in the interior of the domain.

The temperature and specific humidity fields are taken from a radiosonde sounding typical of January from Nairobi, Garisa, Entebbe and Dar-es-Salaam. These data are initialized following Warner et al. (1978).

2.4.2 Boundary Conditions

The lateral boundary conditions used in this study are a set of open boundary conditions following Anthes and Warner (1978). In this specification, the surface pressure and temperature on both the inflow and outflow boundaries are specified as smoothly varying functions of time. This specification prevents any spurious pressure difference across the domain, which would lead to unrealistic net acceleration of the flow. The other variables are extrapolated outward from the interior grid points.

In addition to these conditions we use extended grid mesh such that the boundaries are taken far away from our region of interest. In the vertical, the lower and vertical boundary conditions for vertical velocity component is zero. There are no fluxes of heat, moisture and momentum across the upper boundary.

Table 1 Specified constants in the model

Parameter	Numerical value	Remarks
P_t	300	Pressure at top of model for dry runs
P_t	100	Pressure at top of model for moist runs
ν	0.1	Smoothing coefficient in the time filter
f	$0.0\ S^{-1}$	Coriolis parameter
K_{H0}	$4 \times 10^4 m^2/s$	Constant horizontal diffusion
k	0.35	von Karman's constant
Δt	30S	timestep
l	100m	mixing length
R_{ic}	1.0	Critical Richardson number
K_{zo}	$1\ m^2s^{-1}$	constant vertical diffusion
q_{co}	$5 \times 10^{-4}\ kg\ kg^{-1}$	critical value for onset autoconversion
Δx	20km	grid length
A	0.2	surface albedo over land
	0.06	surface albedo over water
M	1.0	soil moisture over water
	0.1	soil moisture over land
Zo	0.01 cm	surface roughness over water
	10 cm	surface roughness over land

3. RESULTS AND DISCUSSIONS

Four numerical experiments were conducted to study the evolutions of both mesoscale and convective scale systems and the interactions between the two scales of motion and their resultant influence on weather over Kenya in general.

The control experiment was the explicit moisture scheme. All the other results were weighed against the results from this scheme.

3.1 The Results from the Explicit Moisture Scheme

Figure 1 represents the vector and isotach wind field at 1800 h local time from the explicit moisture scheme. The highlights from these simulations show strong convergence over the highlands in the lower layers and divergence in the middle layers of the troposphere. This is indicative of the influence of the mesoscale systems i.e. low-level convergence and divergence aloft. The results show a maximum of 10 m/s in the combined lake breeze/upslope flow on the western slopes of the highlands. A return flow with a maximum wind speed of 6 m/s is noticed aloft at the level of maximum convection. On the eastern sides of the highlands, however, maximum wind speeds of 10 m/s are confined along the ocean coast. This indicates that the sea breeze has no significant influence on the convective activities over the Kenya highlands. The return flow of this regime is deeper but relatively weaker than that of the lake breeze/upslope regimes. Above 400 mb level we, however notice weak wind speeds indicating that the mesoscale influence is perhaps confined in the lower layers of the troposphere. The figure also illustrates the simulation of an extensive cumulonimbus cloud (zig-zag line) in the middle layers of the troposphere. The formation of this cloud is associated with the strong low-level mesoscale convergence and the resultant updraft realised over the Kenya highlands. This is illustrated clearly in figure 2, the vertical velocity field. This figure shows strong upward motion of moist, warm air and relatively weak vertical motions elsewhere. This shows that most of the weather activities are excited by the convergence between the mesoscale systems and interactions between these systems and the convective-scale systems. The level of maximum updraft is favourable for strong convective activity due to the convergence of heat and moisture made available by the moist lake breeze from Lake Victoria.

The maximum updraft above the highlands is surrounded by two weak downdrafts, one on each side. These mesoscale downdrafts represent compensating subsidence around the updraft produced by the lake breeze, upslope flows, and convection. These downdrafts are enhanced by the evaporation of the precipitation and detrainment from the clouds. The maximum velocity in the updraft is 60 mb/h. Fig. 2 also shows characteristic evidence of subsiding air above both Lake Victoria and Indian Ocean during daytime. This subsidence causes clear skies above the water masses, especially above Lake Victoria.

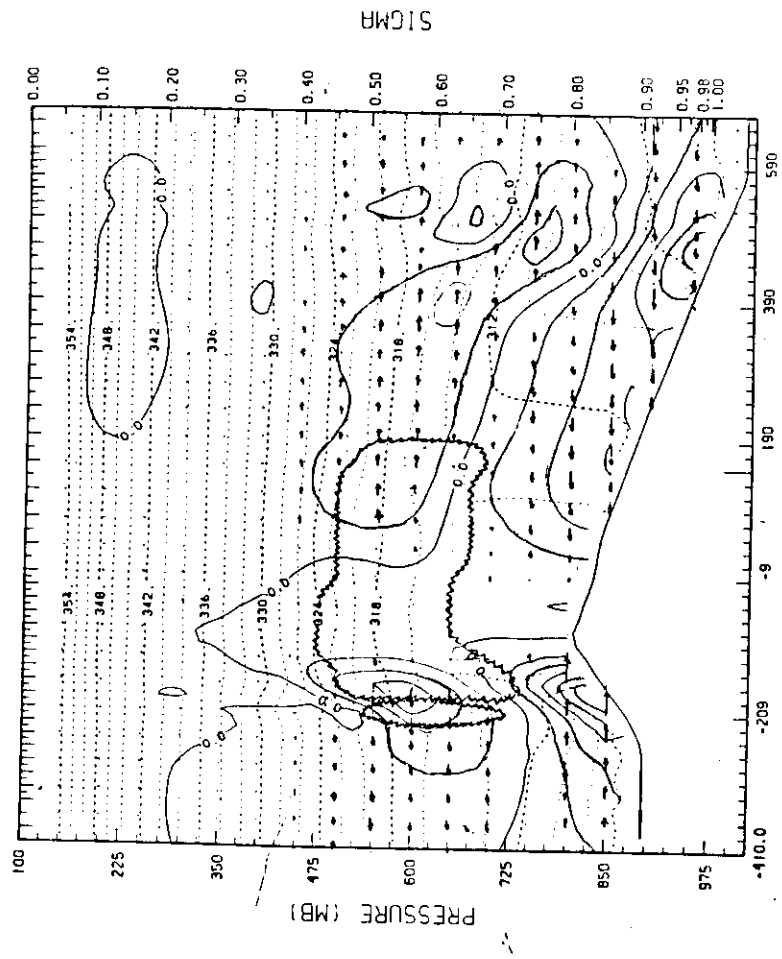

Fig. 1: Vector and Isotach Wind field m/s at 1800h local time (explicit moisture). Contour interval is 2 m/s.

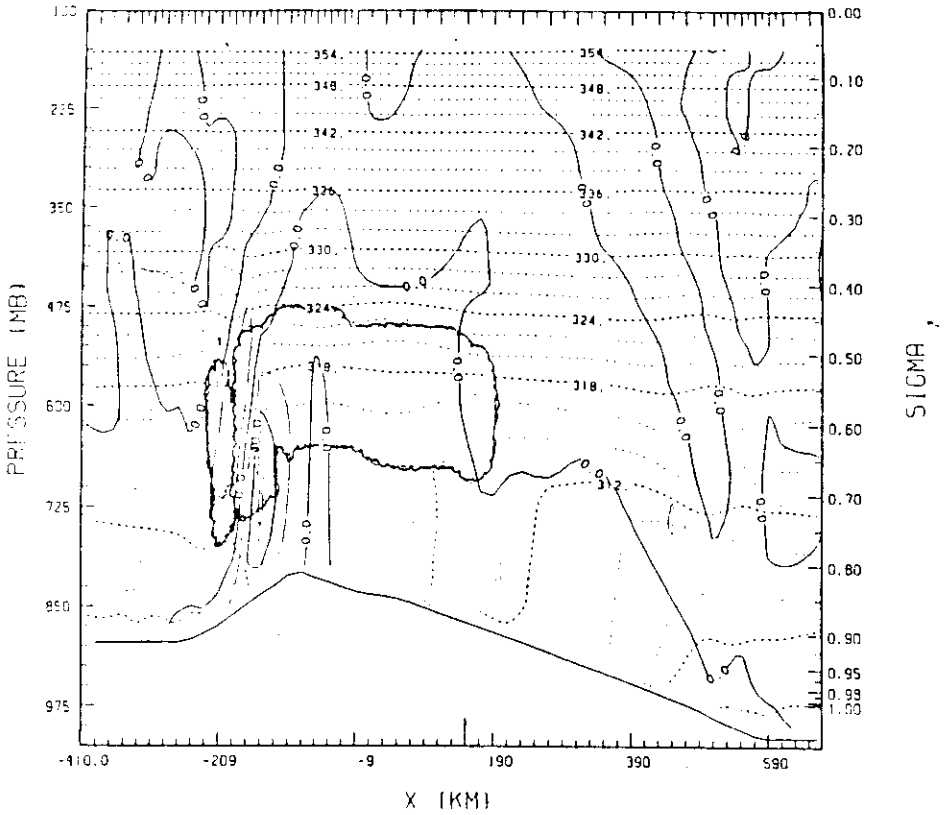

Fig. 2: Vertical velocity (mb/h) at 1800h local time (Explicit moisture). Contour interval is 20 mb/h.

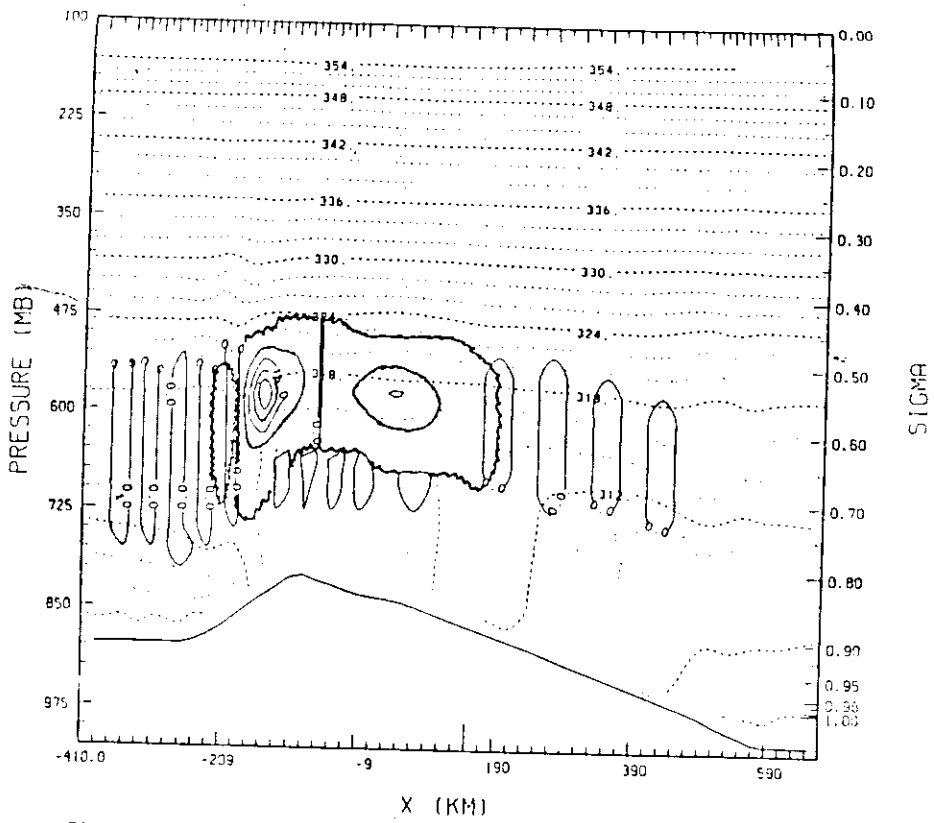

Fig. 3: Condensational Heating (K/D) at 1800h local time (explicit moisture). Contour interval is 8 K/D.

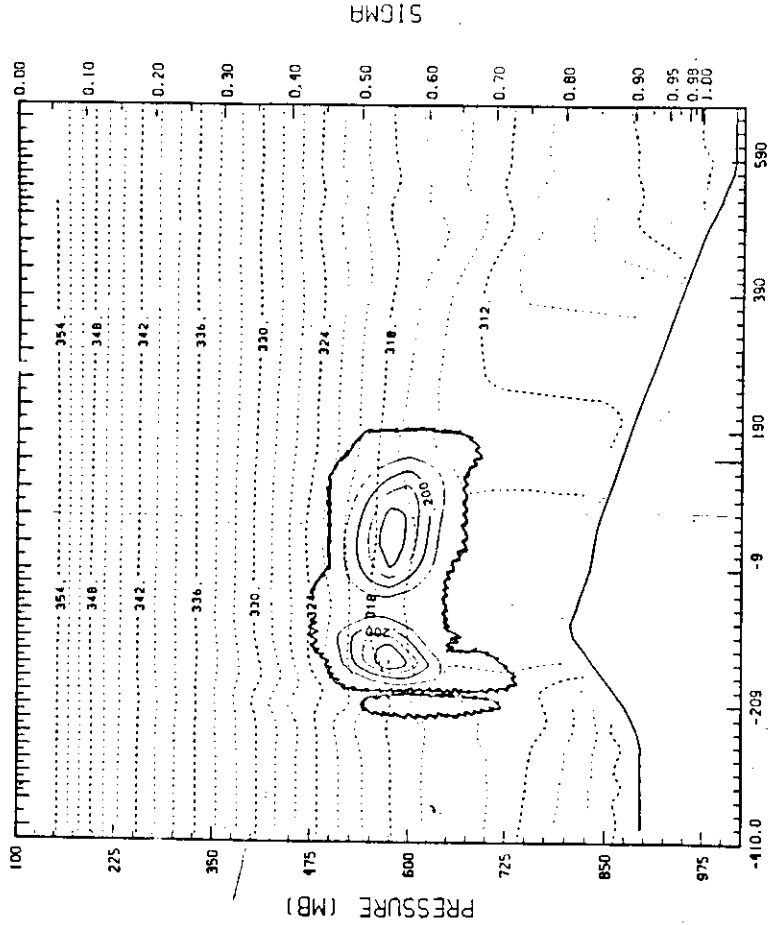

Fig. 4: Cloud water (g/kg) at 1800h local time (explicit moisture). Contour interval is 0.1g/kg.

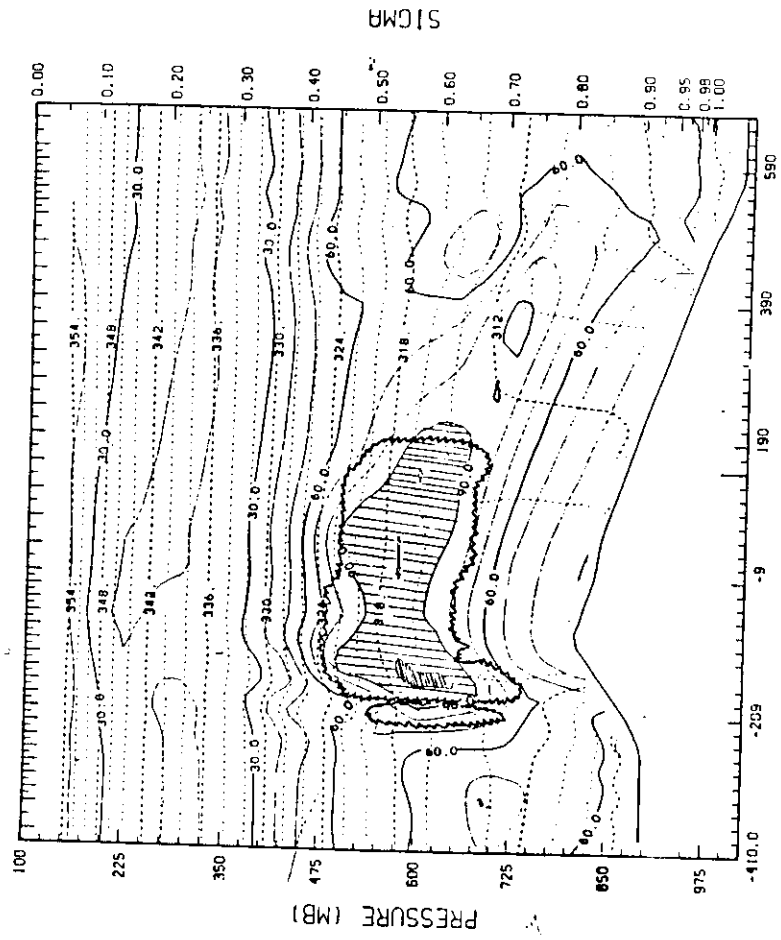

Fig. 5: Relative humidity (RH) (explicit moisture) at 1800h local time. Contour interval is 10%. ||| RH>90% and ≡ RH>100%.

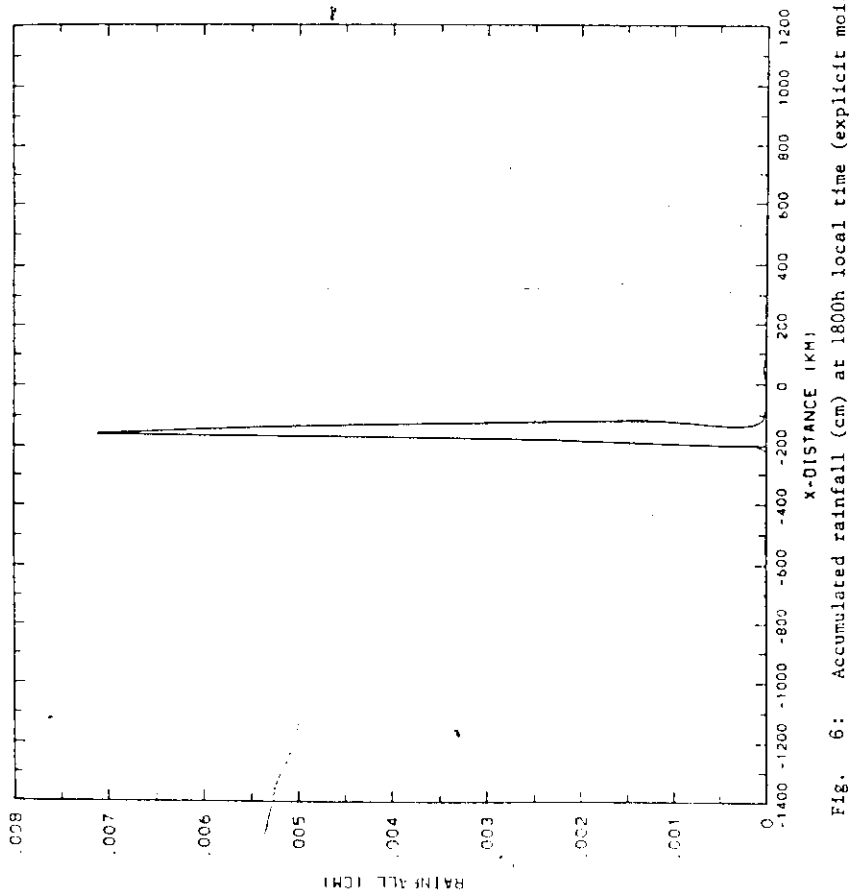

Fig. 6: Accumulated rainfall (cm) at 1800h local time (explicit moisture).

The features discussed above show that condensational heating takes place in areas which are convectively active, such as the Kenya highlands as is shown on Fig. 3. Maximum condensational heating (32 K/day) takes place inside the cloud at the 600 mb level. This is also the level of maximum return flow and just above the level of maximum updraft as discussed above. The cloud water (Fig. 4) maximum level is also realised at the same point confirming strong tropospheric convection normally realised over the Kenya highlands.

The relative humidity field Fig. 5 shows drying in the lower layers above the highlands and moistening in the middle troposphere. This is compatible with the theory that convection transports heat, moisture and momentum to the middle and upper troposphere thereby warming and moistening those levels and hence enhances the outflow from those levels also. The figure also shows that most of the moisture is concentrated over the highlands in the middle layers.

This concentration is favourable for strong precipitation falling over the Kenya highlands as Fig. 6. shows. A maximum rainfall of 0.07 mm was simulated by the model. The foregoing discussion is confirmed by observations over Kenya.

3.2 Results from Cumulus Parameterization Scheme

In this subsection the simulations from cumulus parameterization scheme are discussed and compared with those of the control experiment.

Fig. 7 illustrates the vector and isotach wind field from this scheme at 1800 h local time. This figure shows that the two schemes simulate similar features of the mesoscale and convective-scale systems with minor differences in the magnitudes of the wind field and depths of return flows. The minor changes occur in the lower layers where the combined lake breeze and upslope flow regime have a maximum of 12 m/s as compared to 10 m/s from the explicit moisture scheme (Fig. 1). On the eastern side however the two simulations give equal magnitudes of the flow along the coastal areas.

The slight difference on the wind field (2 m/s) between the two simulations can however cause significant differences in the divergence fields between the schemes. As is well known convection is related to divergence field and hence quite significant differences may appear in other fields which are a function of convection.

Fig. 8 for instance shows the vertical velocity field from the cumulus parameterization scheme. Quite significant difference occurs in the updraft (80 mb/h as compared to 60 mb/h, Fig. 2). This figure also shows stronger downdrafts on each side of the updraft than is shown in Fig. 2. These strong differences in the vertical velocity field would have wide ranging effects in the fields of condensation, humidity, temperature and rainfall.

Fig. 9 shows the field of condensational heating from the cumulus parameterization scheme. As is evident condensational heating is significantly affected by divergence. The maximum condensational heating here is 40 K/day as compared to 32 K/day (Fig. 4). Elsewhere we also notice a wide band of condensational heating featuring a maximum of 16 K/day as compared to that of 8 K/day in the explicit moisture scheme. The scheme also simulates pockets of condensational heating along the eastern slopes of the highlands with maxima of 8 K/day. These differences may also be due to the delay of convection in the explicit moisture scheme due to the storage of cloud water and the evaporation of some of the condensed water.

Simulations of relative humidity show that the cumulus parameterization scheme predicts a more moist upper troposphere than the explicit moisture scheme (compare Fig 10 and Fig. 5). The results are consistent with the observations of the region showing deep cumulonimbus cloud formation almost everyday of the year resulting in frequent thunderstorms/hailstorms and lightning.

Following enhanced convection we notice higher and more widespread precipitation over most of the model domain in cumulus parameterization scheme results (Fig. 11) A maximum rainfall of 0.42 cm is produced as compared to 0.07 mm from explicit moisture scheme. The rainfall field in Fig. 11 also shows a strong banded structure as illustrated in the convergence, vertical velocity and condensational heating fields. This is consistent with the interactions between the mesoscale and convective scale systems illustrated above. The cumulus parameterization scheme however predicts rainfall at the Indian Ocean coastal region. This is inconsistent with observations. This discrepancy is due to the overprediction of rainfall by the cumulus parameterization scheme, which immediately converts a portion of any net moisture to rainfall.

3.3 The Passive Moisture Scheme

In this scheme the moisture variable does not interact with the other dynamic and thermodynamic variables. Two experiments were run using this scheme. In one experiment the model included the lake and the ocean in the runs while in another experiment both the lake and the ocean were excluded from the run. This was done to illustrate the impact of lake/sea breeze on the mesoscale and/or convective-scale systems over Kenya. The model top was at 300 mb.

3.3.1 The Scheme with Lake and Ocean

Fig. 12 shows the vector and isotach analysis from the run with the lake and ocean at 1800 h local time. We notice a maximum wind speed of 9 m/s on the lake side as compared to 10 m/s in the explicit moisture scheme (Fig. 1). Little or no changes are noticed elsewhere except for a stronger return flow on the eastern side of the highlands (5 m/s as compared to 4 m/s in Fig. 1). These small differences in the horizontal wind field have been shown, however to have very strong influences in the vertical wind field and other related convection aspects. Fig. 13 shows that the maximum velocity in the updraft is 52 mb/h as compared to 60 mb/h in the explicit moisture (Fig. 2).

The other minor differences between the two schemes are found in the depths of the lake breeze/upslope flow. In the explicit moisture scheme, it reaches a height of 720 mb while in the dry scheme it only reaches 750 mb. This result is also attributed to the interaction between mesoscale and convective scale systems.

3.3.2 The Dry Scheme without Lake and Ocean

Fig. 14 illustrates the major differences between the experiments with and without lake and ocean. While the flow pattern and major features remain the same, the magnitudes are significantly different. In the upslope regime from the western side of the highlands, the maximum wind speed is only 4 m/s as compared to 9 m/s in Fig.12 and on the eastern slopes the maximum is only 6 m/s as compared to 10 m/s in Fig. 12 The return flows are also relatively weaker.

The influence of sea/land breeze circulations on the development of clouds and other small-scale systems has been sited in the past by several researchers Gentry (1950), Day (1953), Gentry and Moore (1954) and Hsu (1969) found from observation studies that sea and land breezes influenced thunderstorms or shower occurrence. Pielke (1974) used a three-dimensional numerical model and found that the afternoon showers over South Florida were related to the sea breeze convergence zone. In a recent study Okeyo (1987), the author showed that Lake Victoria was responsible for most of the moisture and energy needed for the development of hailstorms over the Kenya highlands.

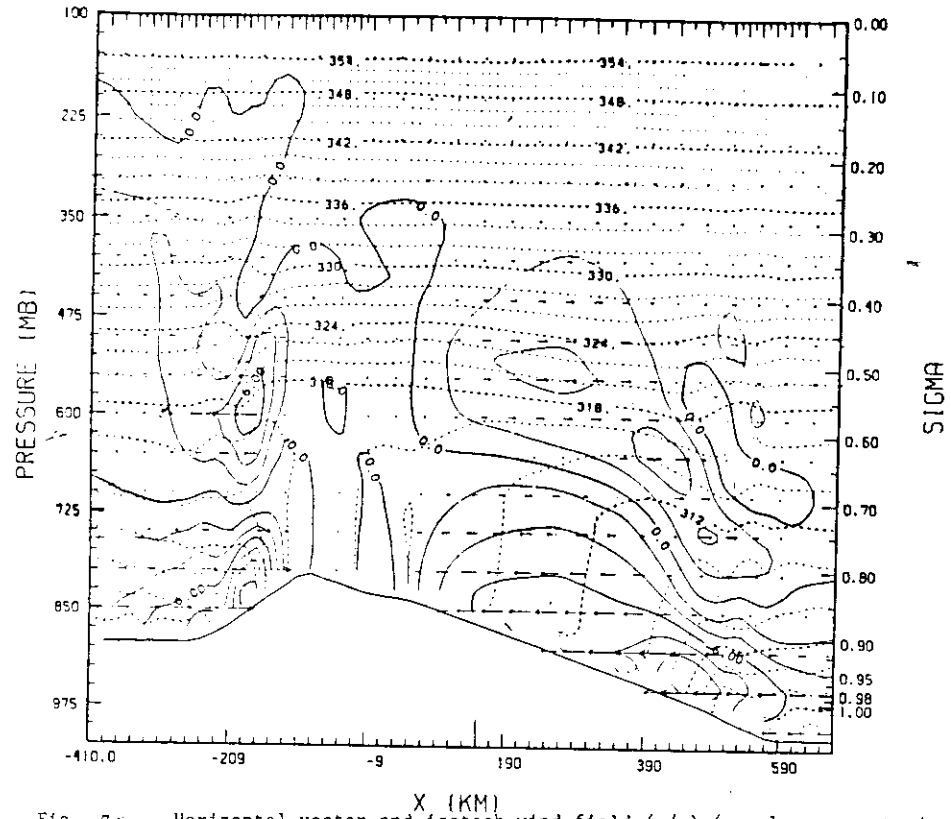

Fig. 7: Horizontal vector and isotach wind field (m/s) (cumulus parameterisation)

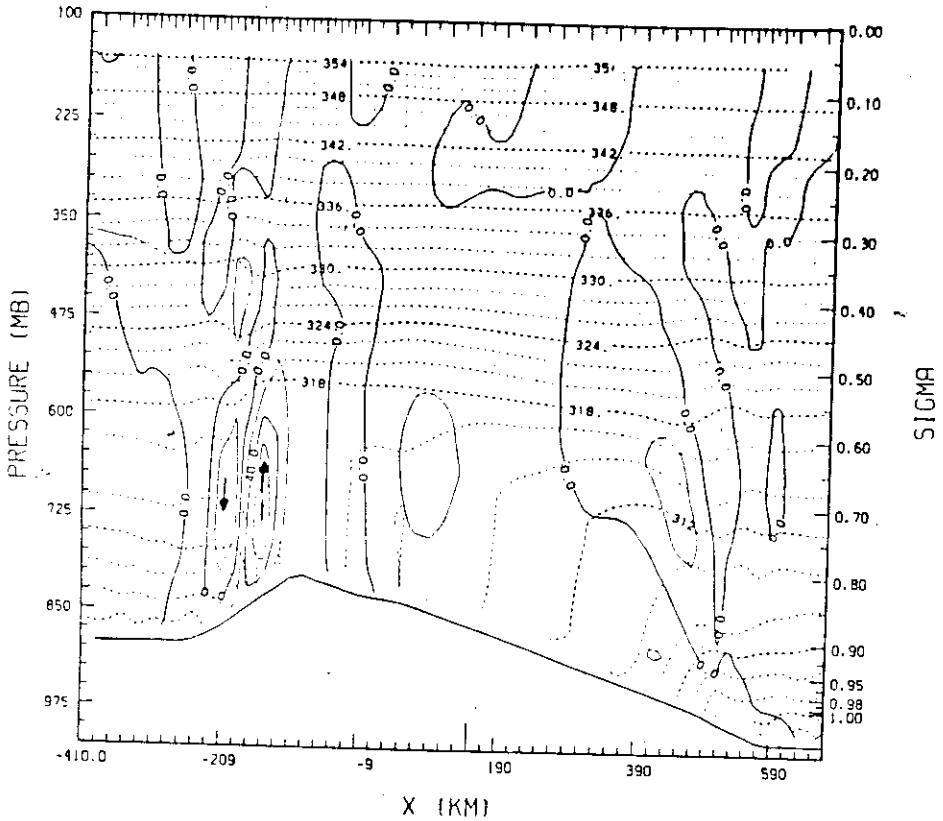

Fig. 8: Vertical velocity (mb/h) at 1800h local time (cumulus paramterisation). Contour interval is 20 mb/h.

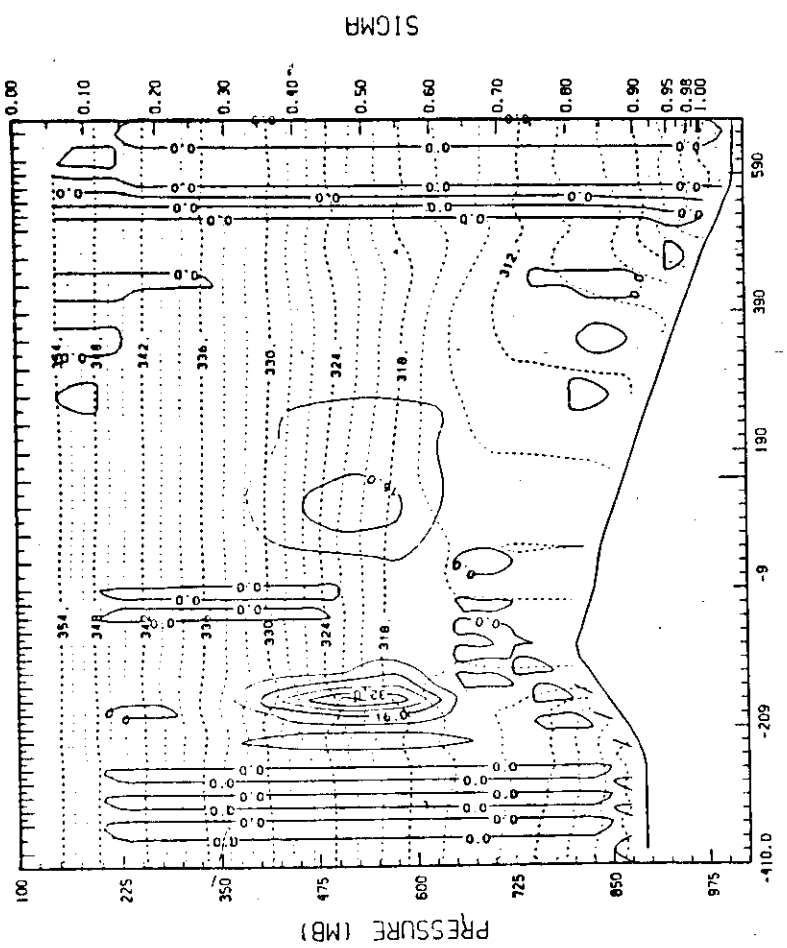

Fig. 9: Condensational heating (K/D) at 1800h local time (cumulus parameterisation). Contour interval is 8 K/D.

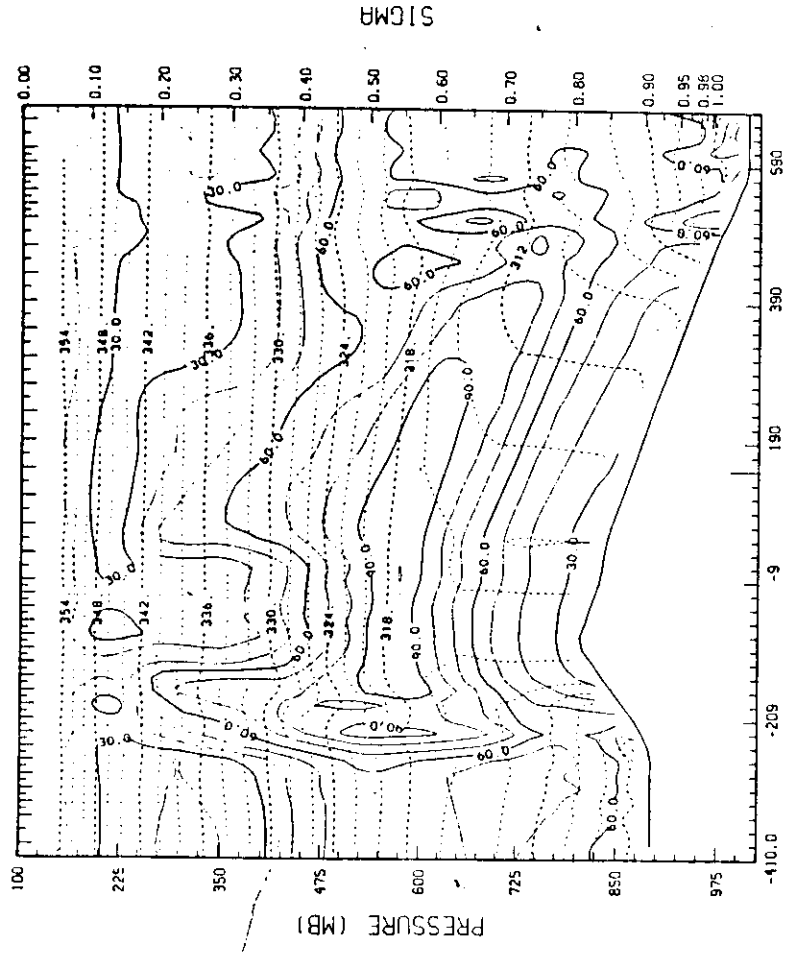

Fig. 10: Relative humidity field (%) at 1800h local time (cumulus parameterisation). Contour interval is 10%.

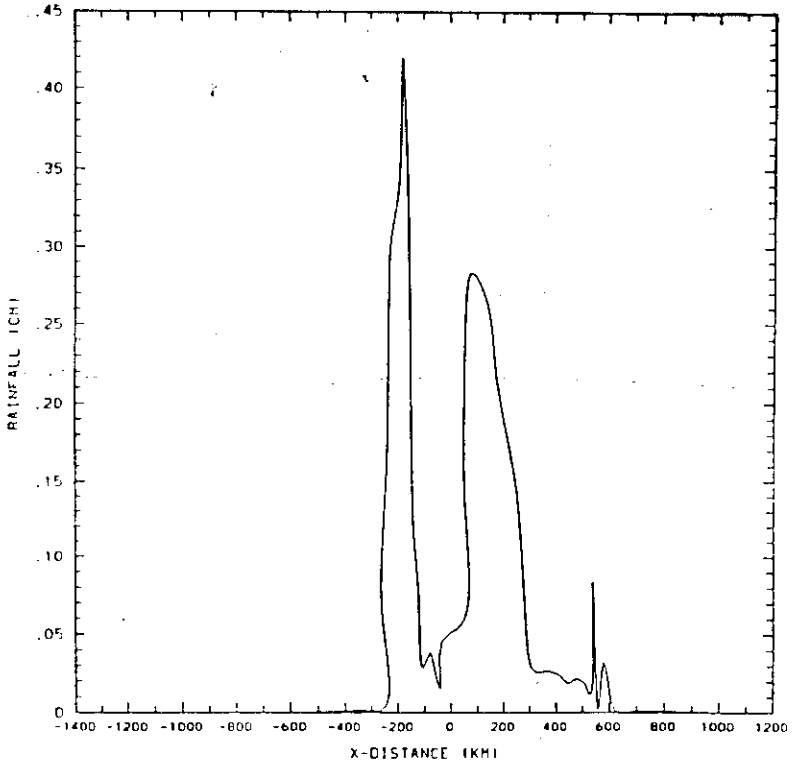

Fig. 11: Accumulated rainfall (cm) at 1800h local time (cumulus parameterisation).

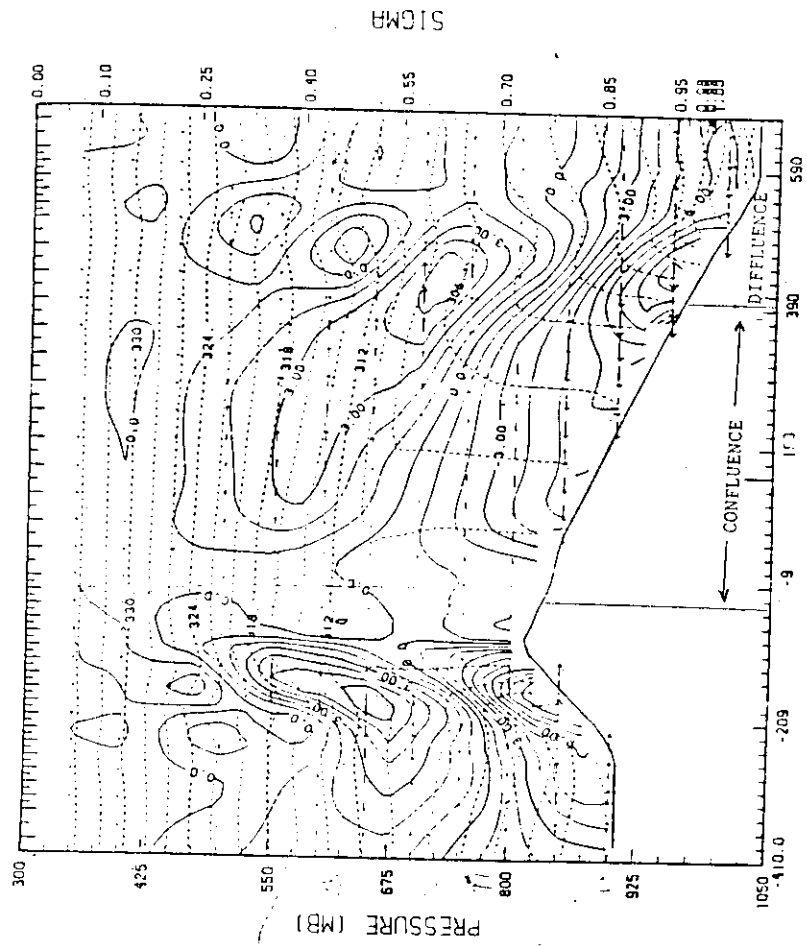

Fig. 12: Vector and isotach wind field m/s at 1800h local time (Passive moisture scheme). Contour interval 1 m/s.

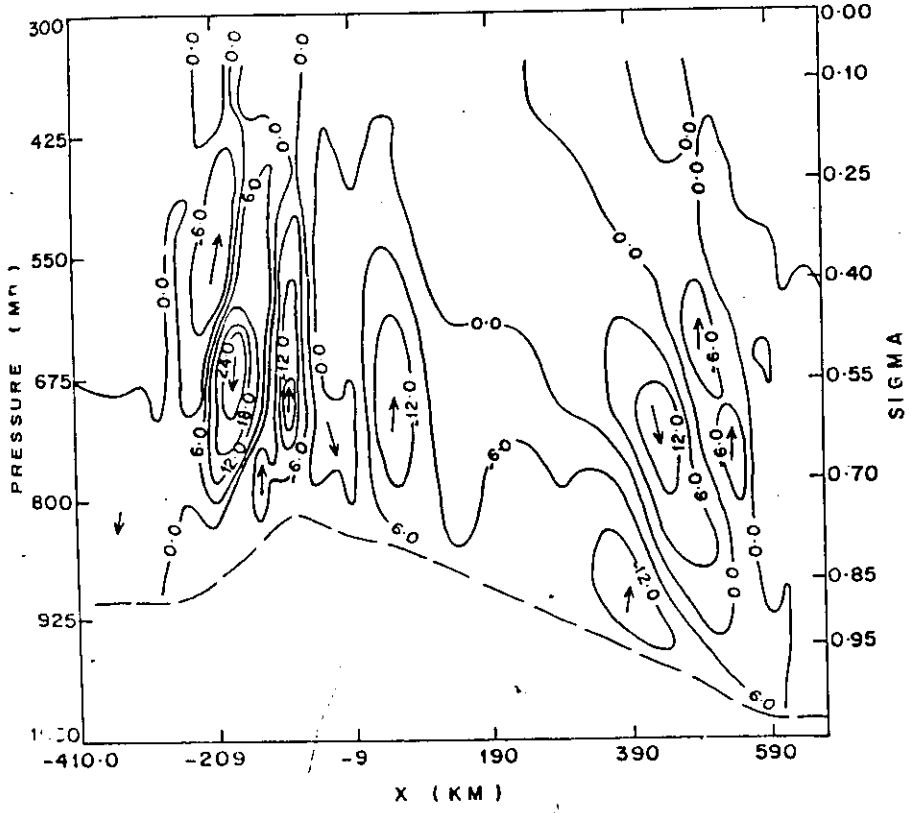

Fig. 13: Vertical Velocity (mb/h) at 1800h local time (passive moisture). Contour interval is 6 mb/h.

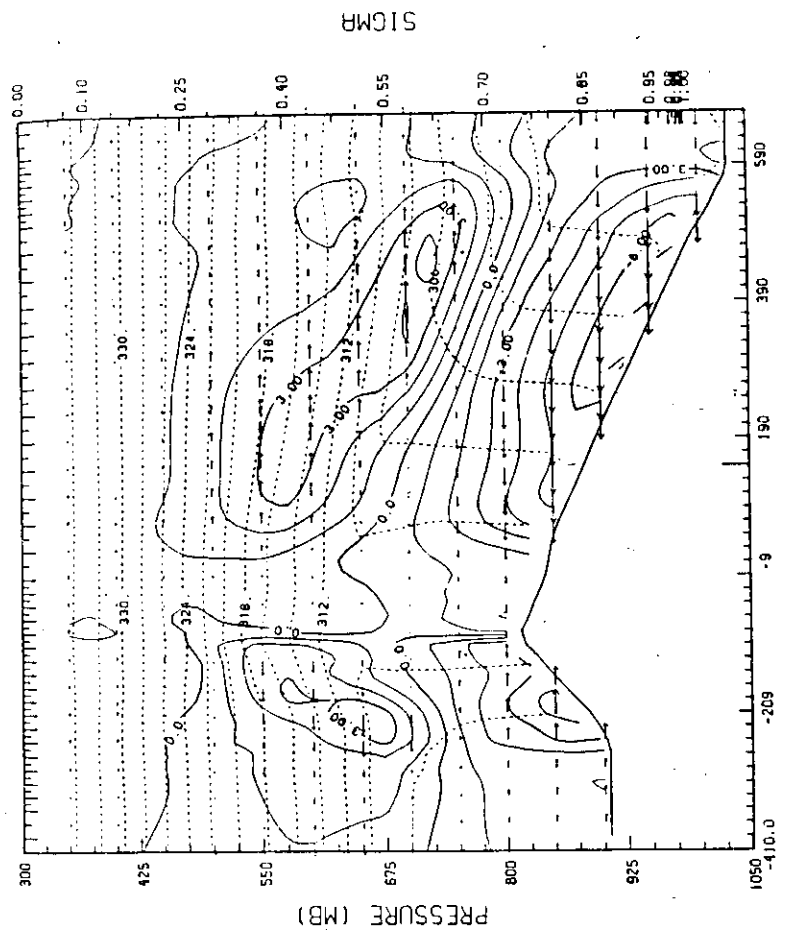

Fig. 14: Horizontal vector and isotach wind field (m/s) at 1800h local time (experiment AL). Contour interval is 1 m/s.

SUMMARY AND CONCLUSIONS

We have used a two-dimensional numerical model to simulate the mesoscale systems that often influence the weather patterns in Kenya. The mesoscale systems of significance are lake/sea and land breezes and valley and mountain winds. Four experiments have been carried out to test the impact of the above mesoscale systems on weather over Kenya in particular and over the tropical regions in general. These four experiments include: explicit moisture scheme (control experiment), cumulus parameterisation scheme, passive moisture scheme and the removal of both Lake Victoria and Indian Ocean from the runs.

The results show that in comparing the explicit moisture scheme and the cumulus parameterisation scheme, results from the cumulus parameterisation scheme are found to be closer to observations than those from explicit moisture scheme. The cumulus parameterisation scheme produced stronger vertical velocities and hence stronger condensational heating since condensational heating is coupled to the vertical velocities. The cumulus parameterisation scheme also simulated more rainfall expecially above the Kenya highlands than the explicit moisture scheme. The cumulus parameterisation scheme however, simulated rainfall along the coastal areas of the Indian Ocean during day-time which is not supported by observations. This was due to the overprediction of rainfall by the cumulus parameterisation scheme, which immediately converts a portion of any net moisture to rainfall.

The results from the experiment which excluded Lake Victoria and Indian Ocean gave wind speeds almost half those that included the two water masses. These results show that the combined lake/sea and land breezes and valley and mountain winds strong influence on weather over Kenya.

The results from this study will have very strong influence on the energy and water budgets and on the improvement of weather forecasting over Kenya.

ACKNOWLEDGEMENTS

This work was done partly in the Department of Meteorology, University of Nairobi, Kenya and partly at National Centre for Atmospheric Research Boulder, Colorado, U.S.A. The author is therefore indebted to the two institutions for providing funds and facilities to carry out the research. I am greateful to the staff at National Centre for Atmospheric Research in general who provided the computer facilities and expertise to enable this work to be completed. The author is particularly thankful to Dr. Richard Anthes whose advice was important towards the completion of this research.

REFERENCES

Anthes, R.A., 1977: A cumulus parameterisation scheme utilizing a one-dimensional cloud model. Mon. Wea. Rev., 105, 270-286 .

-----, and T.T. Warner, 1978: Development of hydrodynamic model suitable for air pollution and other mesometeorological studies. Mon. Wea Rev., 106, 1045-1078.

-----, E.-Y. Hsie and Y.-H. Kuo, 1987: Description of the Penn State/ NCAR mesoscale model version 4(MM4). NCAR Technical Note NCAR/TN-282 + STR, National Centre for Atmospheric Research, Boulder, CO. 80307, 66pp.

Asai, T., 1965: A numerical study of the Airmass transformation over the Japan sea in winter J. Meteor. Soc. Japan, 43, 1-15.

Asnani, G.C. and J.H. Kinuthia, 1979: Diurnal variation of precipitation in East Africa. Kenya Met. Dept. Research Report No. 8/79, 1-58.

Asselin, R., 1972: Frequency filter for time integration. Mon. Wea. Rev. 100, 487-490.

Brown, J. and K. Campana, 1978: An economical time-differencing system for numerical weather prediction. Mon. Wea. Rev., 106, 1125-1136.

Chaggar, T.C., 1977: Geographical distribution of monthly annual mean frequency of thunderstorm days over Eastern Africa. EAMD Tech. Note No. 26.

Day,S., 1953: Horizontal convergence and occurrence of summer precipitation at Miami, Florida. Mon. Wea. Rev. 81, 155-161.

Emannuel, K.A., 1982: Inertial instability and mesoscale convection systems. Part II: Symetric CISK in a baroclinic flow. J. Atmos. Sci., 39, 1080 - 1097.

Estoque, M.A. 1961: A theoretical investigation of the sea breeze. Quart J. Roy Meteor. Soc., 87, 136 - 146.

--------, 1962: The sea breeze as a function of the prevailing synoptic situation. J. Atmos Sci., 19, 244-250.

Flohn, H., 1970: Climatic effects of local winds in tropical and subtropical latitudes symp. Tropical Met., Honolulu, Hawaii.

Fraederick, K. 1972: A simple climatological model of the dynamics and energetics of nocturnal circulation at Lake Victoria. Quart. J. Roy Met Soc., 98, 322-335.

Gentry, R.C., 1950: Forecasting local showers in Florida during summer. Mon. Wea. Rev., 78, 41-49.

----------, and P.L. Moore, 1954: Relation of local and general wind interaction near the sea coast to the time and location of airmass showers. J. Meteorol., 11,507-511.

Hsie, E.-Y., 1983: Frontogenesis in a moist atmosphere. PhD Thesis, The Pennsylvania State University.

Hsu, S.A., 1969. Mesoscale structure of Texas coast sea breeze. Report No. 16, NSF Grant EA-367X, University of Texas at Austin, College of Engineering, Atmospheric Science Group, 237 pp.

Kessler, E., 1969: On the distribution of continuity of water substance in atmospheric circulations. Meteor. Monogr. 27, Amer. Meteor. Soc., 84 pp.

Keyser, D. and R.A. Anthes, 1982: The influence of planetary boundary physics on frontal structure in Hoskins-Bretherton horizontal shear model. J. Atmos. Sci., 39, 1783-1802.

Kuo, Y. -H. and R.A. Anthes, 1984a: Accuracy of diagnostic heat and moisture budgets using SESAME -79 field data as revealed by observing system simulation experiments. Mon Wea. Rev., 112, 1466-1481.

------- and ------1984b: Mesoscale budgets of heat and moisture in a convective system over central United States. Mon. Wea. Rev., 112, 1482-1497.

-------and ----1984c: Semi-prognostic tests of Kuo-type cumulus parameterisation schemes in extratropical convective systems. Mon. Wea. Rev., 112, 1498-1509.

Liu, J.Y. and H.D Orville, 1969: Numerical modelling of precipitation and cloud shadow effects on mountain induced cumuli. J. Atmos. Sci., 26, 1061-1074.

Moroz, W.J., 1967: A lake breeze on the eastern shore of Lake Michigan, Observations and Model. J. Atmos Sci., 24, 337-335.

Okeyo,A.E., 1982: A two -dimensional numerical model of the mesoscale systems over Kenya. MSc Thesis University of Nairobi of Nairobi, 244pp.

----------, 1987: The influence of Lake Victoria on the convective activities over the Kenya highlands. Special volume of J. Meteor. Soc. Japan, WMO/IUGG NWP symposium, Tokyo, 4-8 August 1986, 689-695.

Orville, H.D., and F.J. Kopp, 1977: Numerical simulation of the life history of a hailstorm. J. Atmos Sci., 34, 1596-1618.

Pearce, R.P., 1955: The calculation of sea-breeze circulation in terms of the differential heating across the coastline. Quart. J. Roy. Meteor. Soc. 81, 351-381.

---------, 1962: A simple theory of the generation of sea breezes. Quart. J. Roy. Meteor. Soc., 88, 20-29.

Pielke, R.A., 1974: A three-dimensional numerical model of the land and sea breezes over South Florida. Mon. Wea Rev., 102, 115-139.

Sansom, H.W. and S. Gichuiya, 1971: Hailstorms in the Kericho area. EAMD Tech. Memo No. 22.

Shuman, F.G. and J.B. Hovervamalle, 1968: An operational six-layer primitive equation model. J. App. Meteor. 7, 525-547.

Simpson, J. and V. Wiggert, 1969: Models of precipitating cumulus towers. Mon. Wea. Rev., 97, 471-489.

Warner, T.T., R.A. Anthes and A.L. McNab, 1978: Numerical simulations with a three-dimensional mesoscale model. Mon. Wea. Rev., 106, 1079-1099.